

Numerical Modeling of an Earthquake-induced Landslide Considering the Strain-softening Characteristics of the Clayey Loam



A. Wakai

Gunma University, Kiryu, Japan

K. Matsushita

Former Graduate student of Gunma University, Kiryu, Japan

T. Fukushima

Graduate student of Gunma University, Kiryu, Japan

SUMMARY:

In the present study, a strain-softening constitutive model for clayey loam is applied to simulate an earthquake-induced catastrophic landslide that occurred at the time of the 2011 disaster of the Great Tohoku and Kanto Earthquake in Japan. In this case, the upper part of the slope had slid downward for more than 50m. Only the shear-strength degradation of the clayey loam layers in the slope could cause such a long-distance traveling failure. To investigate the strain-softening characteristics of the material, a series of laboratory tests involving undisturbed block samples is performed. The stress-strain relationships under cyclic loading are numerically modelled as the proposed elasto-plastic constitutive model, which is also used in the numerical simulation for the landslide, based on the dynamic finite element method. Accordingly, the observed phenomena are appropriately simulated by the proposed numerical method.

Keywords: Slope, Finite Element Method, Loam, Strain-softening, Constitutive Model

1. INTRODUCTION

In the present study, a strain-softening constitutive model for clayey loam is applied to simulate an earthquake-induced catastrophic landslide that occurred at the time of the 2011 disaster of the Great Tohoku and Kanto Earthquake in Japan. In this case, the upper part of the slope had slid downward for about 100m. Only the shear-strength degradation of the clayey loam layers in the slope could cause such a long-distance traveling failure.

In the following chapters, first of all, the observed phenomena related to the objective landslide are introduced in detail, followed by the discussions in geomorphological, geological and geotechnical points of view. Those essential facts are used for the numerical simulations in order to clarify the exact mechanisms of triggering the landslide during the earthquake. Finally, the obtained results and a few additional conclusions are summarized briefly.

2. ANALYSIS FOR AN EARTHQUAKE-INDUCED LANDSLIDE

As for the objective landslide (seen in the map in **Fig. 2.1**), the upper part of the slope had slid downward for more than 50m. Such a long-distance traveling failure is one of the typical cases of landslides occurred in the hill area around the Shirakawa-City in Fukushima Prefecture at the time of the earthquake.

2.1. Geomorphological and geological characteristics

In this case, a slope in the ridge greatly deformed and the debris covered the adjacent houses and road. The travel distance of the debris was found more than 50 m. The material has been strongly disturbed and it was mainly composed of softened clayey loams containing a large number of light-coloured

stiffer loamy lumps which have been crushed into around 0.3 to 1 m in diameter (**Fig. 2.2**). The apparent sedimentation angle in the slope, which might have been formed by the previous landslide events as well as orderly volcanic ash fall, was a little gentler than the inclination of the surface. The dip angle was measured by the several tephra layers observed in the exposed vertical cliff of about 10 m tall at the upper part of the suffered slope.

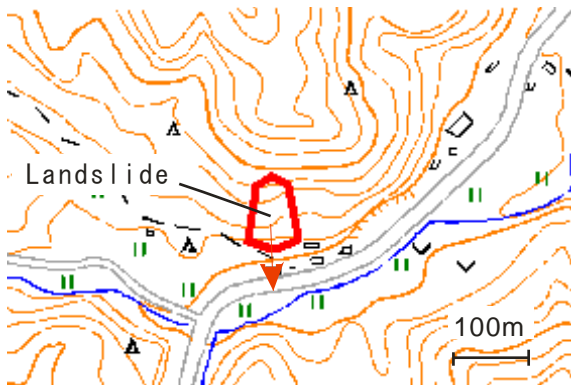


Figure 2.1. Objective landslide at Okanouchi in Japan



Figure 2.2. Whole view of the landslide



Figure 2.3. Exposed planar slip surface with clayey loam including a lot of small stone pieces



Figure 2.5. Sub layers with a lot of stone pieces in the clayey loam cliff.

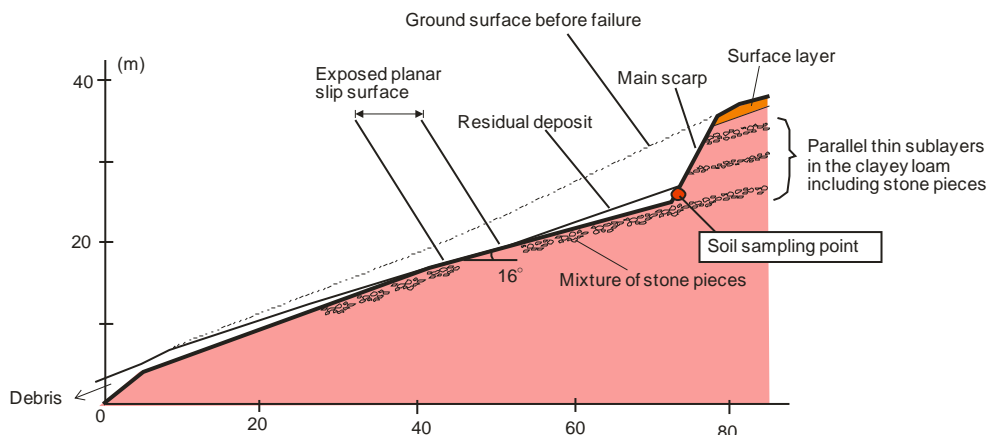


Figure 2.4. Geological formations at the centre cross section in the slope

A portion of the scratched planar slip surface was exposed at the centre of the collapsed area (Fig. 2.3). The material at the slip surface appears to be a clayey loam including a lot of small stone pieces about 0.2 to 0.5 m in diameter, which may have been produced from tuffaceous rocks in the upstream area of this mountain. The inclination of the planar surface is approximately 16°, which is almost the same as the dip angle.

The geological formations and the observed slip surface at the centre cross section in the slope are shown in Fig. 2.4. The maximum depth of the sliding block is about 10 m below the slope surface. Because the suffered-slope topography is asymmetrical in the right and left direction, the thickness of the sliding block in the west (right-hand side) part is larger than that shown in this figure.

The volcanic cohesive soil or loam as a dominant material in the slope contains a few types of loamy layers with different stiffness and particle sizes, inserting a thin pumice layer as well. In the exposed cliff, there also can be found three thin layers with a lot of small tuffaceous stone pieces (Fig. 2.5), suggesting this slope has experienced several times of large-scale landslide events up to now. This is probably related to the tephra of about 0.1 million years ago was found in the middle of the cliff, the sliding block may contains the sediments older than the tephra.

The observed planer slip surface passed between the following two layers; the lower loam layer reinforced with mixture of small tuffaceous stone pieces and the upper clayey loam layer that may be easily softened by seismic excitation. The stress concentration effect around the stiffness-changing depth might promote such a catastrophic landslide induced by the strength degradation of clayey loam due to cyclic softening.

Fig. 2.6 is a close-up of a block soil sample used to investigate the mechanical properties of the material around the slip surface. This block sample was harvested at the foot of the exposed vertical cliff. The material is a brown-coloured clayey loam and rich with fine materials. The particle size distribution curve for the investigated soil/material is shown in Fig. 2.7. The natural water content and the liquid limit of the material are 83.9% and 97.8 %, respectively. Those values are closer to each other and it implies that the material can easily behave like a fluid after sudden strength degradation due to the seismic disturbance. The estimated sensitivity ratio from unconfined compression tests was about 3.0, which was not a particularly low value. The cohesion and the internal friction angle at the peak strength under the natural water content conditions were found to be 7.1 kN/m² and 49.3°, respectively.



Figure 2.6. Sampling of undisturbed block of clayey loam in the cliff

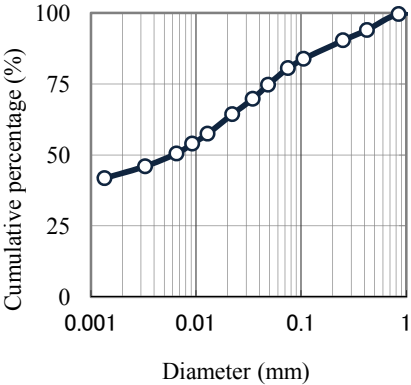


Figure 2.7. Particle size distribution of the sampled clayey loam

2.2. Cyclic loading characteristics of the problematic clayey loam

A series of the undrained cyclic triaxial tests of undisturbed specimens were performed as well. The soil specimens were kept to have natural water content, which means all the tests have been carried out

under unsaturated conditions to represent the field conditions. The initial effective confining pressure in the tests was set as 100 kN/m^2 , that corresponds to the stress level around the bottom of the sliding block. **Fig. 2.8** shows one of the examples of the observed results in the cyclic triaxial tests. It can be seen that the apparent shear resistance gradually decreased, like liquefaction of loose sands under cyclic loading, while the excess pore water pressure ratio has been kept to be much lower than 1.0. It suggests that the undrained shear strength of the unsaturated clayey loam in the slope can be decreased without the remarkable accumulation of the excess pore water pressure during the earthquake. This fact may decline the application of simple liquefaction models in effective stress formulations exclusively for saturated soils, in the numerical simulation for this event.

The apparent liquefaction strength curve for $DA=5\%$ measured by the cyclic triaxial tests, i.e., the relationships between the amplitude of shear stress ratio and the number of cycles to achieve the axial strain amplitude of 5%, are shown in **Fig. 2.9**. Also, the strain dependency on the equivalent shear deformation modulus and the damping ratio were observed in the series of undrained cyclic triaxial tests, as shown in **Fig. 2.10**. In these figures, the simulated curve by the UW softening model in total stress formulations (Wakai et al. 2010) is compared to the observed results. In the model, the effect of the excess pore water pressure under cyclic loading is modelled as the decreasing functions of the undrained shear strength parameters with the accumulated shear strain. The material parameters used for the simulation are summarized as the material named ‘‘Clayey loam with softening’’ in **Table 2.1**. The simulated curves agree with the results obtained by the laboratory tests.

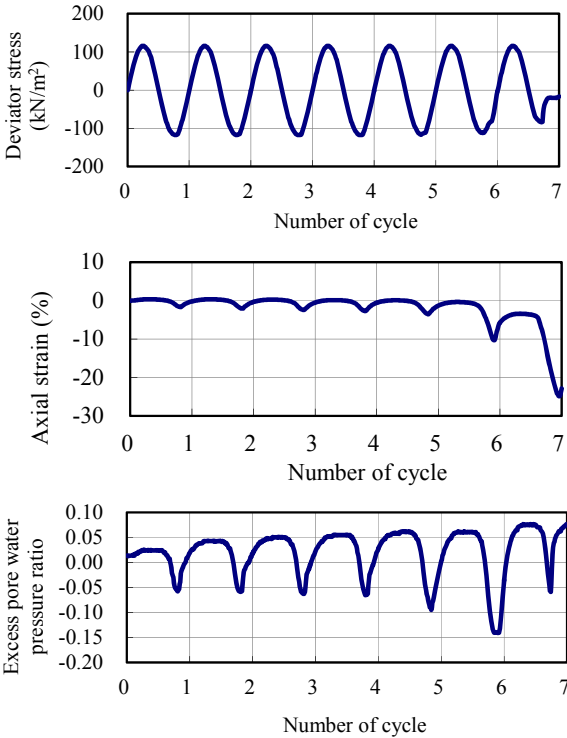


Figure 2.8. An example of the observed result of the cyclic triaxial tests for the clayey loam with the natural water content ($S_r = 85.3\%$)

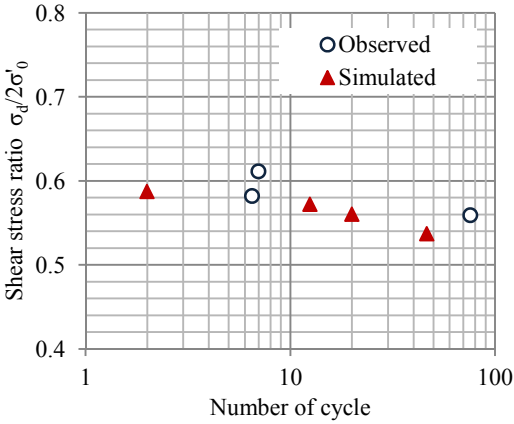


Figure 2.9. Observed and simulated apparent liquefaction strength curve of the clayey loam

2.3. Finite element simulation for the objective landslide

Based on the above numerical modelling, the finite element simulation for the investigated landslide has been performed. The assumed geological structure used in the analysis is shown in **Fig. 2.11**. The discretized finite element meshes (8-nodes) are also overdrawn in the same figure. The calculated acceleration and displacement histories at Point A in **Fig. 2.11** are shown in detail later herein. As for the clayey loam layer with a possibility of cyclic softening, the UW softening model with the above

parameters is adopted, while the lower layer with a lot of stone pieces is modelled as the original UW model without cyclic softening (Wakai & Ugai 2004). The parameters for other materials are shown in **Table 2.1** as well.

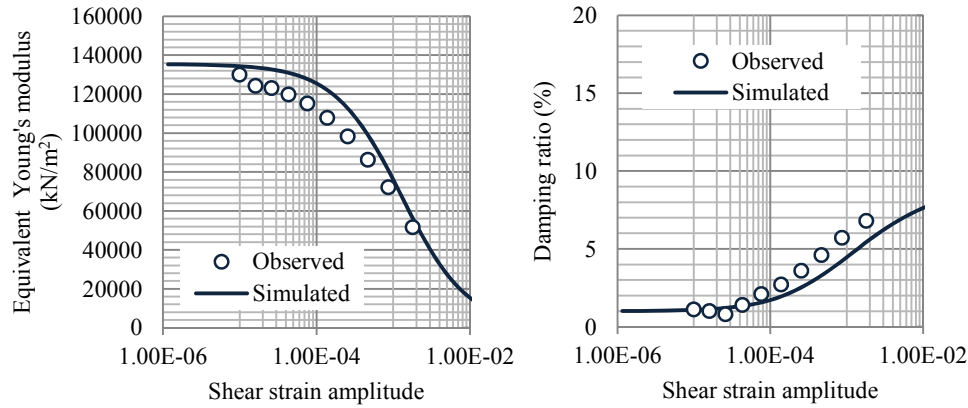


Figure 2.10. Observed and simulated dynamic deformation characteristics of the clayey loam

Table 2.1. Analytical parameters used for the simulation of the clayey loam behaviour by the UW softening model

Materials	Surface soil	Clayey loam		Sand and gravel
		With softening	Without softening	
Young's modulus $E(\text{kN/m}^2)$	100000	$13540 \times (p_0)^{0.5}$ p_0 : Initial confining pressure		1000000
Poisson's ratio ν	0.4	0.4	0.4	0.3
Cohesion $c(\text{kN/m}^2)$	50	49.3		100
Internal friction angle $\phi(\text{deg})$	0	7.1	45	45
Dilatancy angle $\psi(\text{deg})$	0	0		0
$b \cdot \gamma_{cs}$ (Parameter for damping)	6.28	2.5		1.1
n (Parameter for damping)	1.58	2.2		2.8
Unit weight $\gamma(\text{kN/m}^3)$	15	15.28		18
Residual strength ratio τ_{rs} / τ_{c0}	—	0.5	—	—
A (Parameter for softening)	—	10	—	—

Rayleigh Damping	
α	β
0.0571	0.000578

The amplitude of the input waves at the base has been adjusted so that the corresponding horizontal component of the observed records at K-net Shirakawa by NIED should be realized at the ground level in the finite element meshes. The time history of the input horizontal acceleration is shown in **Fig. 2.12**. While, **Fig. 2.13** shows the time histories of horizontal acceleration and displacement at the surface of the slope in the sliding block, namely, Point A in **Fig. 2.11**. The figure indicates that a catastrophic failure occurred in this case. The horizontal displacement became approximately 11 m at the conclusion of the earthquake. Note that this value continued to increase even after the earthquake motion ended. During continuing the movement, the acceleration response continues to be unstable.

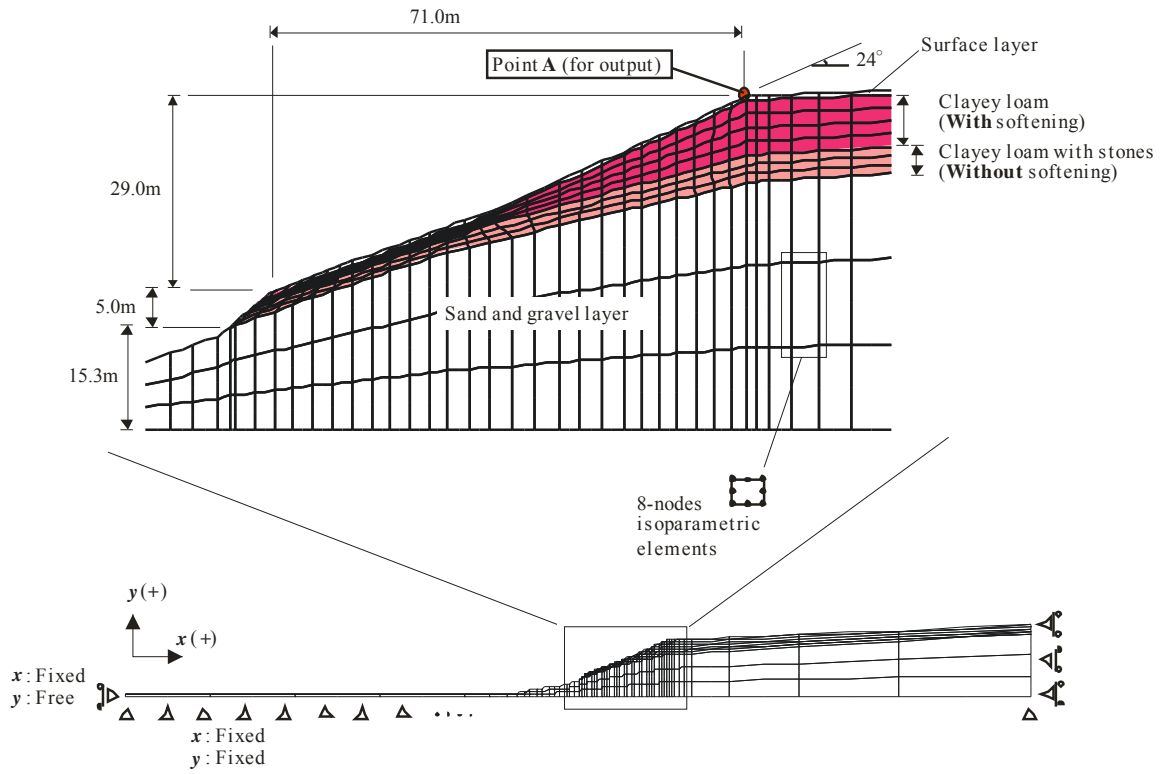


Figure 2.11. Discretized finite element meshes with material assignment

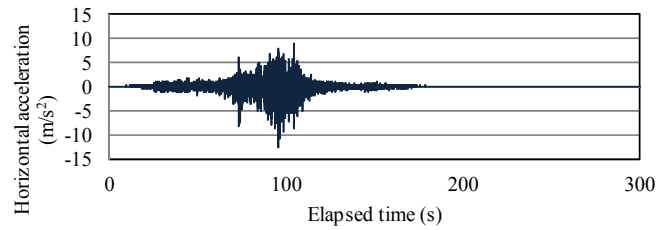


Figure 2.12. Time history of the input horizontal acceleration

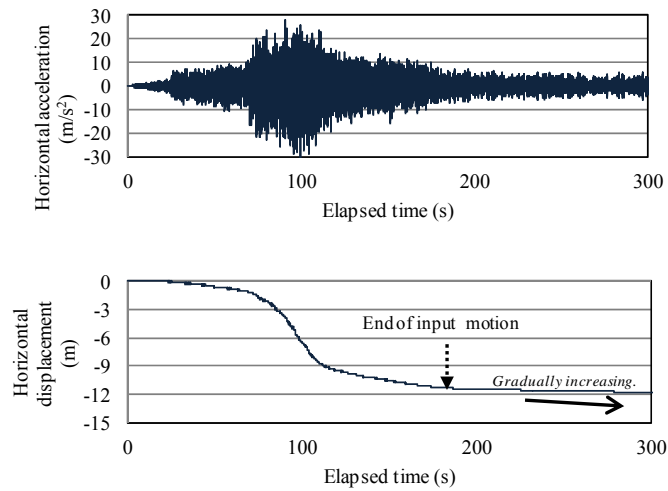


Figure 2.13. Time histories of horizontal acceleration and displacement at Point A in Fig. 2.11

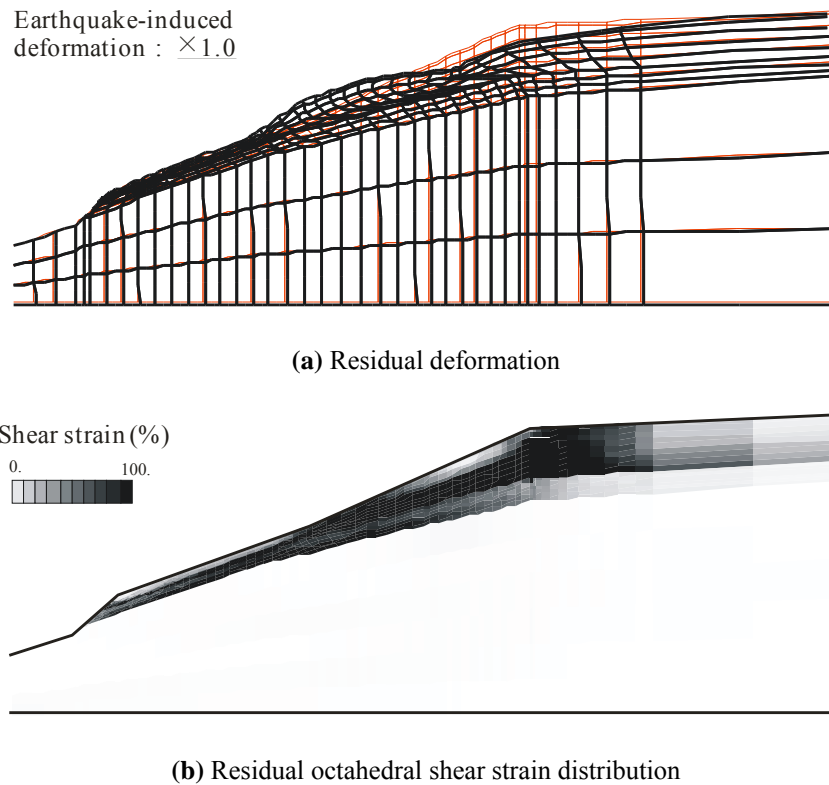


Figure 2.14. Residual deformations and the shear strain distribution at 130 s after the end of the seismic motion

The residual deformations and the shear strain distribution at 130 s after the end of the seismic motion are shown in **Figs. 2.14(a) and (b)**, respectively. The long-distance movement of the sliding block along the upper end of the stiffer layer is clear as presented in the figures. This result is in agreement with the actual phenomenon. Note, however, that the predicted velocity of the sliding mass may not have sufficient accuracy. In order to simulate precisely the sliding behaviour after having started such high-speed motion, it would be better to improve the numerical model for the friction and damping at the bedding plane, which will be a subject for future investigation. Although an exact simulation of the high-speed movement cannot be obtained, this analysis provides information and guidelines for judging the occurrence of such a catastrophic failure.

3. CONCLUSIONS

In the present study, the observed phenomena in an earthquake-induced catastrophic landslide, occurred at the time of the 2011 disaster of the Great Tohoku and Kanto Earthquake in Japan, are appropriately simulated by the dynamic finite element method where the stress-strain relationships under cyclic loading for the clayey loam are numerically modelled as the proposed elasto-plastic constitutive model. It was shown that the shear-strength degradation of the clayey loam layers in the slope caused such a long-distance traveling failure and the detailed investigation for such problematic soils in natural slopes would be so important to make it improved the seismic resistance of slopes especially in suburban areas in Japan.

ACKNOWLEDGEMENT

The authors would like to thank Dr. Tsutomu Soda, President-director of Institute of Tephrochronology for Nature and History Co., Ltd. and Prof. Takehiko Suzuki, Tokyo Metropolitan University, for their great help for the identification of volcanic tephra in the slope. Special thanks extended to Mr. Takashi Yoshida and other laboratory staffs at The Core-Lab, OYO Corporation for their help in conducting the laboratory tests under unsaturated conditions for the clayey loam sampled from the site. The authors appreciate their great efforts which helped us in this study.

REFERENCES

- Wakai, A. and Ugai, K. (2004). A simple constitutive model for the seismic analysis of slopes and its applications. *Soils and Foundations* **44:4**, 83-97.
- Wakai, A., Ugai, K., Onoue, A., Kuroda, S. and Higuchi, K. (2010). Numerical Modeling of an earthquake-induced landslide considering the strain-softening characteristics at the bedding plane. *Soils and Foundations* **50:4**, 515-527.